

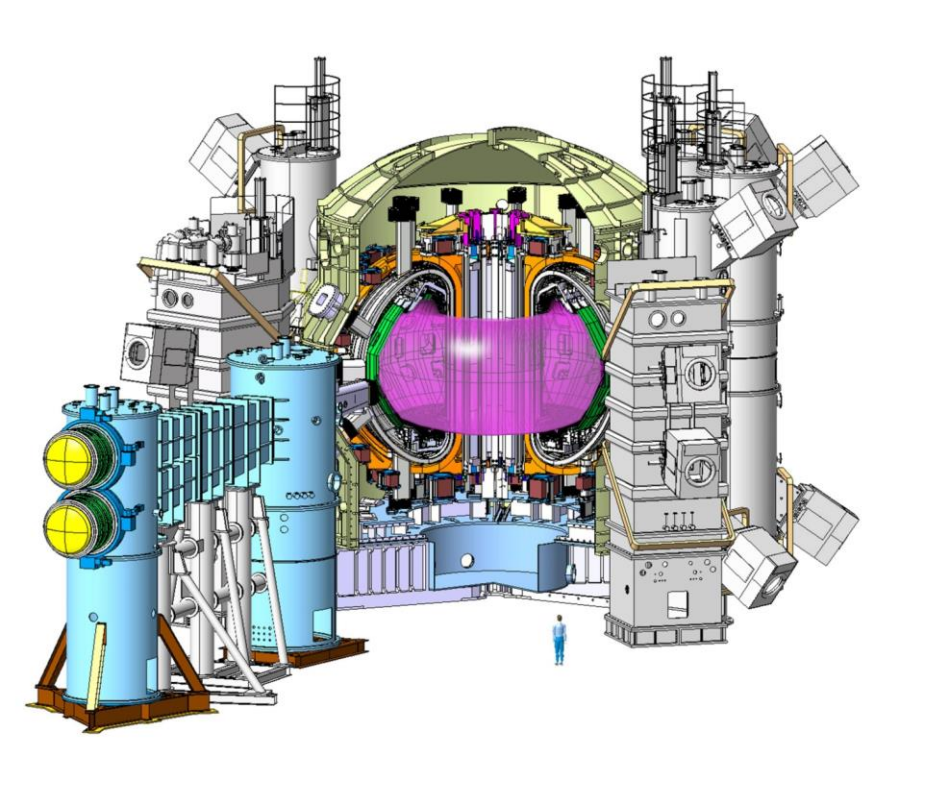
# DEVELOPMENT OF EQUILIBRIUM CONTROL SIMULATOR AND EXPERIMENTAL VALIDATION OF ADVANCED ISO-FLUX EQUILIBRIUM CONTROL DURING THE FIRST OPERATIONAL PHASE OF JT-60SA

S. Inoue, Y. Miyata, S. Kojima, T. Wakatsuki, M. Takechi, Y. Ohtani, Y. Ko, M. Yoshida, H. Urano, and T. Suzuki



### **JT-60SA** project





- Joint international fusion experimental device being built and operated by Japan and Europe, in Naka, Japan
- Main characteristics:
  - Large (~3.0 m major radius) superconducting devise
  - High power (41 MW) and long pulse (~100 s) capability
- Target plasma parameters:
  - High current (5.5 MA) and highly shaped ( $\kappa_X \sim 1.9$ ,  $\delta_X \sim 0.5$ ) plasmas with long sustainment (~100 s)

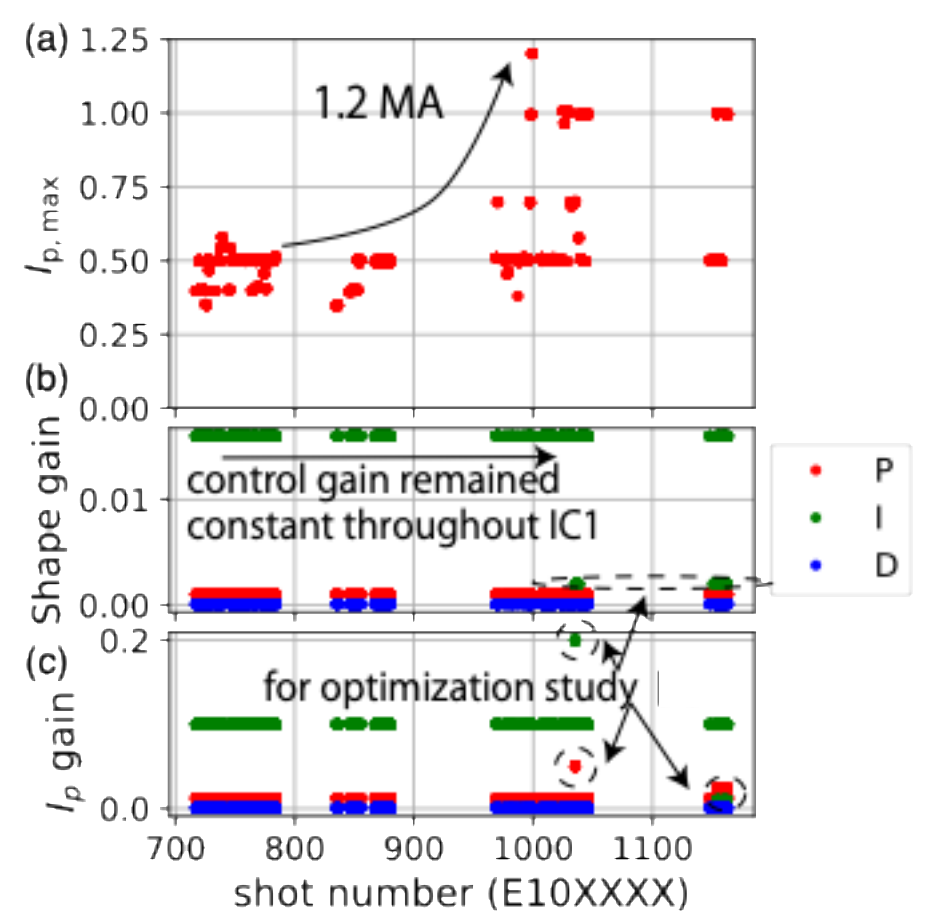
Address key scientific and technological issues for ITER and DEMO



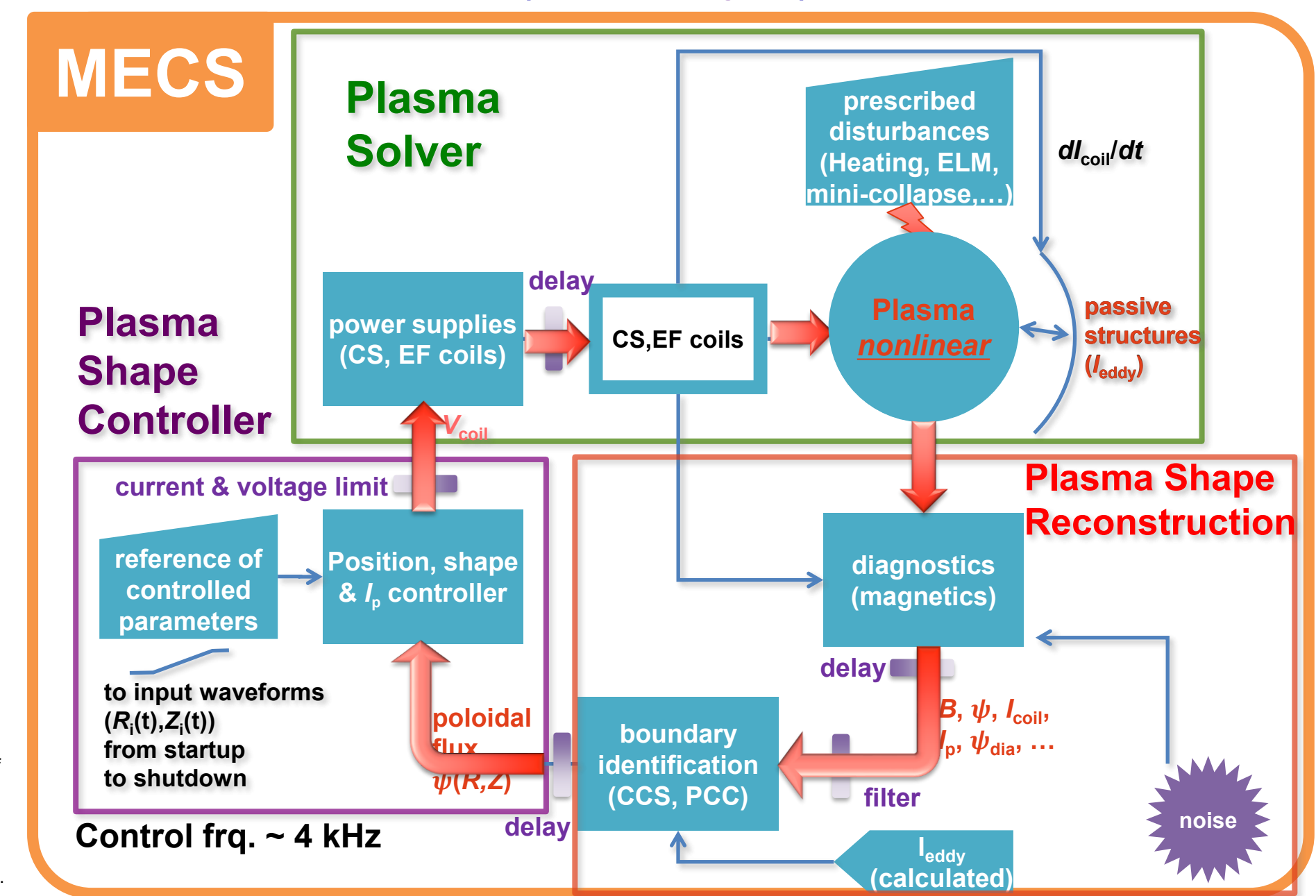
**Equilibrium control is essential** 

### Pre-studied control gain worked without any modification

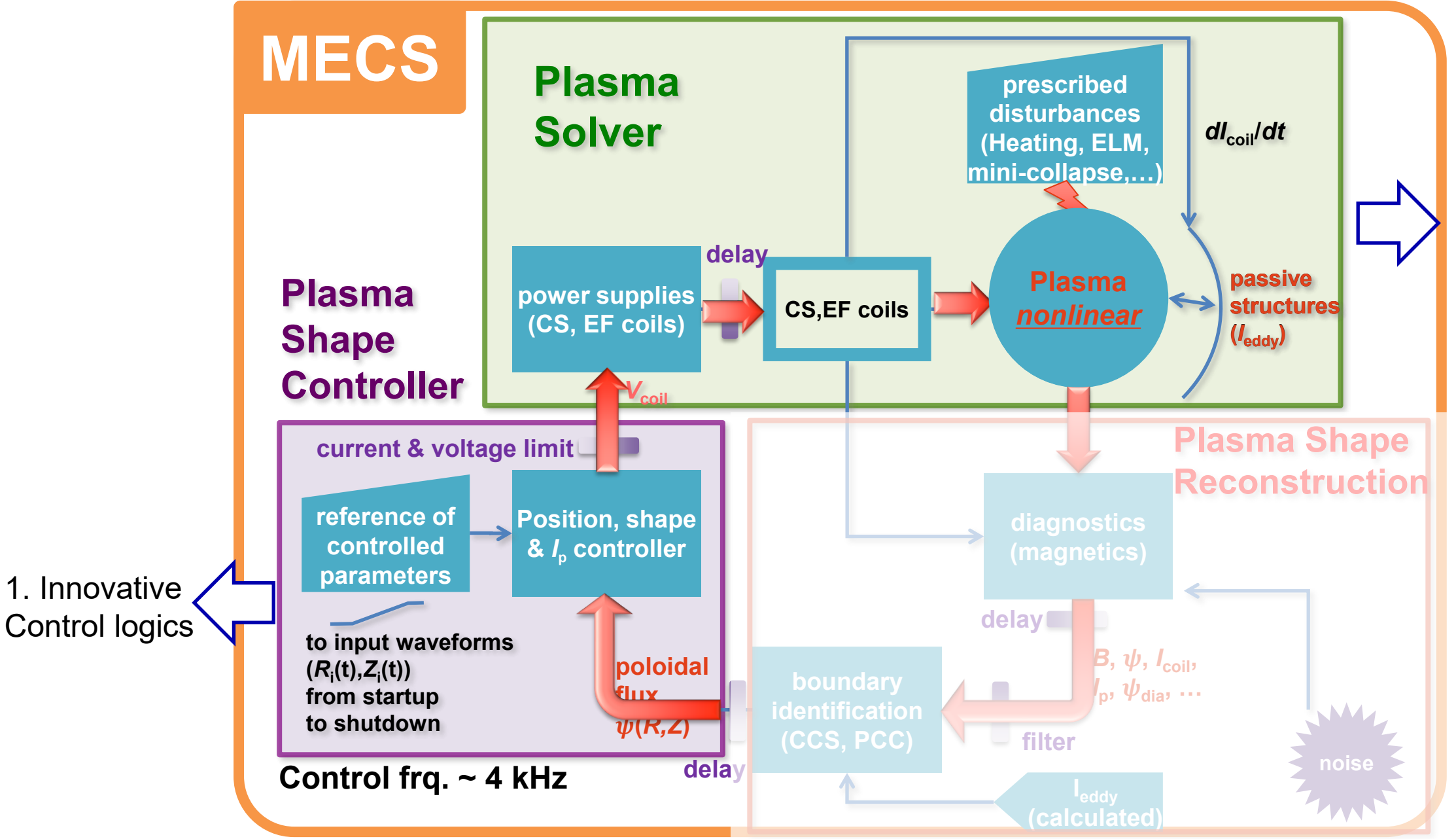




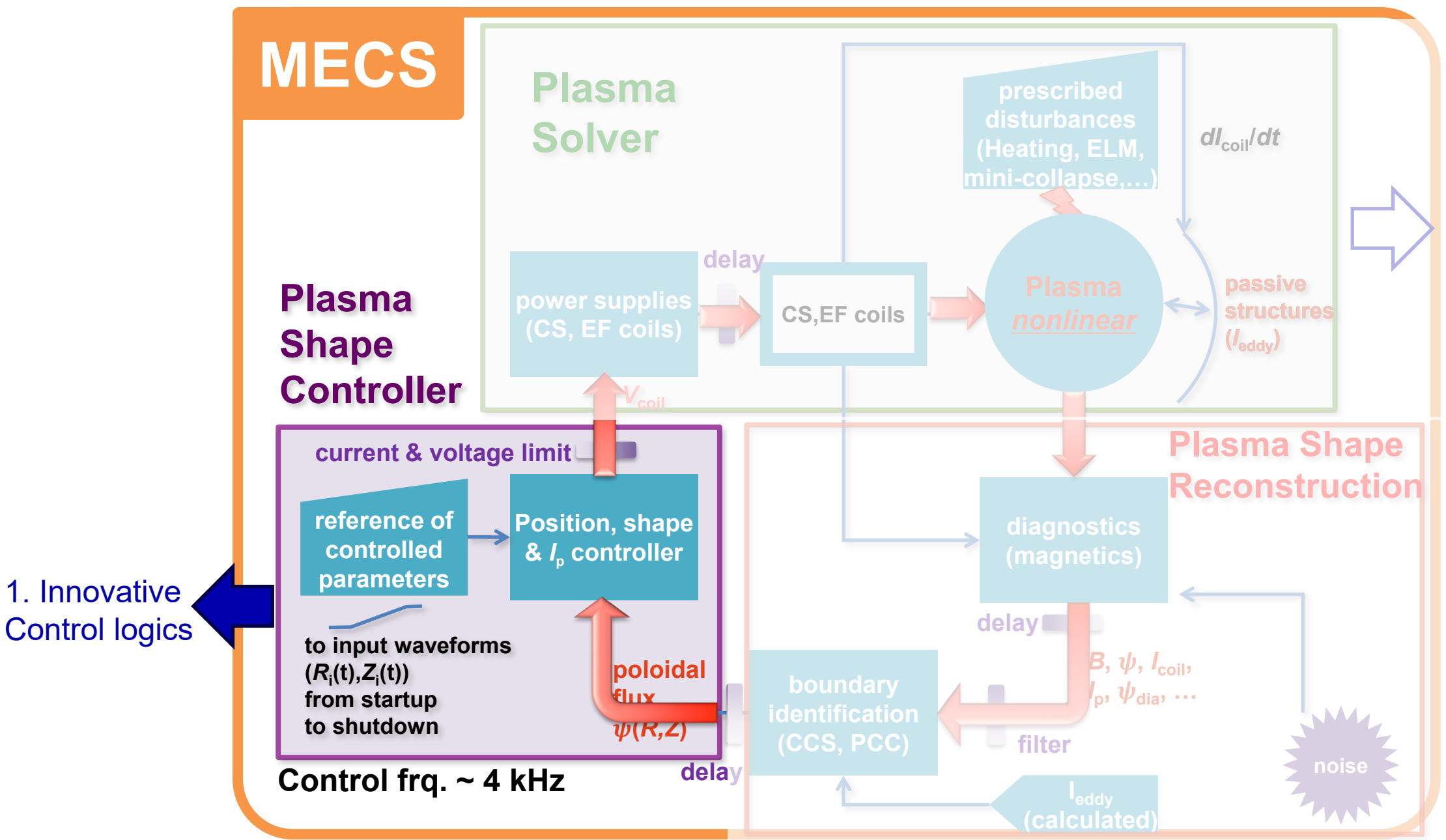
- In the first operation (integrated commissioning, IC) in 2023, ~200 shots with plasma were performed
  - 1.2 MA diverted plasma
  - Pre-studied control gains by simulator, MECS, worked without any modification
- Key question: Why did the predictions work so well?
- Objective: to reveal the essential physics required for accurate prediction of equilibrium control
   → directly linked to fusion performance
- Achievement: first identification of the nonlinear response/axisymmetric field amplification of plasma



<sup>1</sup> Y. MIYATA, T. SUZUKI, T. FUJITA, S. IDE, and H. URANO, "Development of a Simulator for Plasma Position and Shape Control in JT-60SA," Plasma Fusion Res **7**(0), 1405137–1405137 (2012).

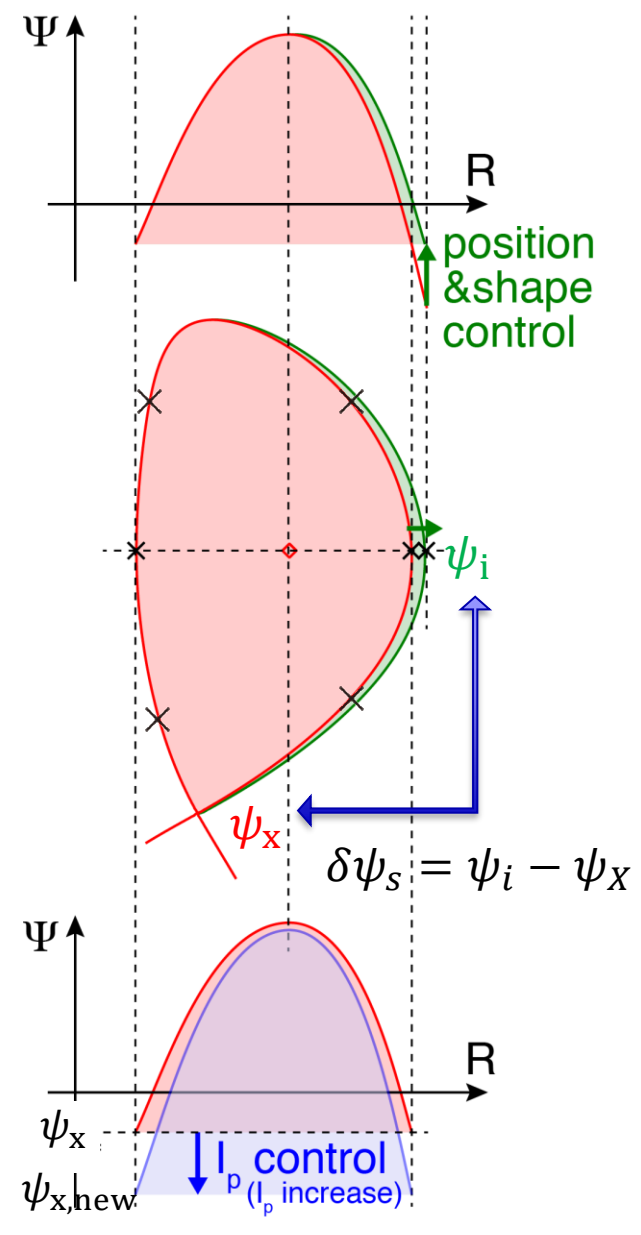


2.Key physics for vertical instability



2.Key physics for vertical instability





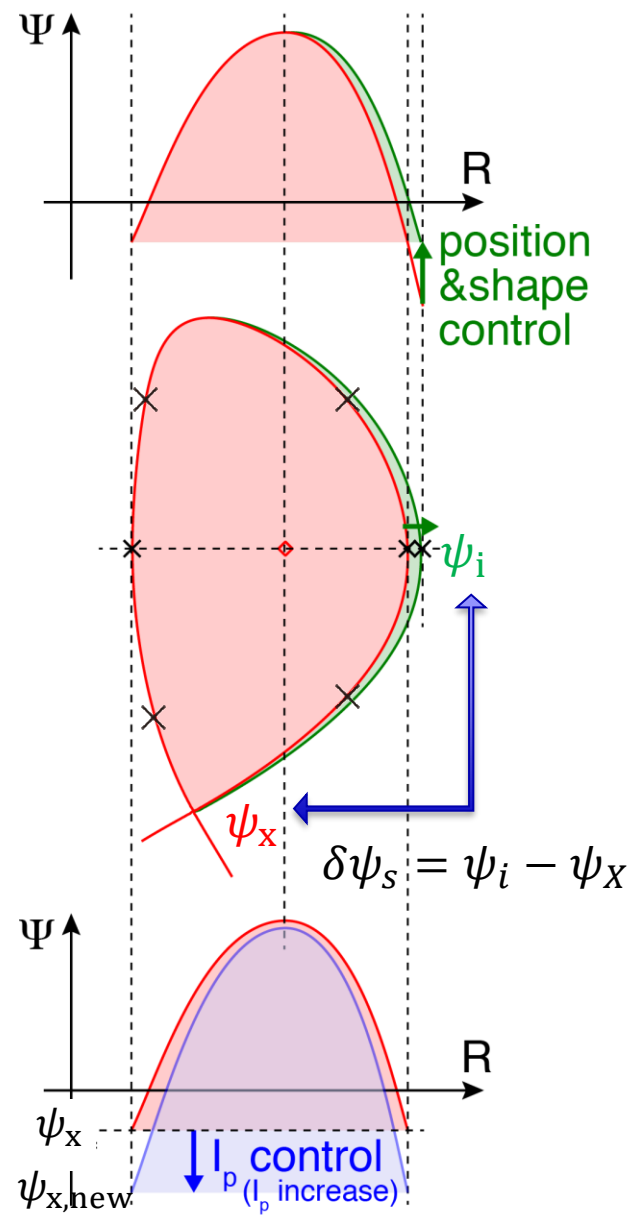
#### **ISO-FLUX control**

(**Shape**)  $\delta \psi_{\rm S}$ : X-point and prescribed control points

(Ip)  $\delta \psi_{\rm X}$ : Offset of all control points

$$\delta \boldsymbol{\psi} = \delta \boldsymbol{\psi}_{S} + \delta \boldsymbol{\psi}_{X}$$





#### **ISO-FLUX control**

(**Shape**)  $\delta \psi_{\rm S}$ : X-point and prescribed control points

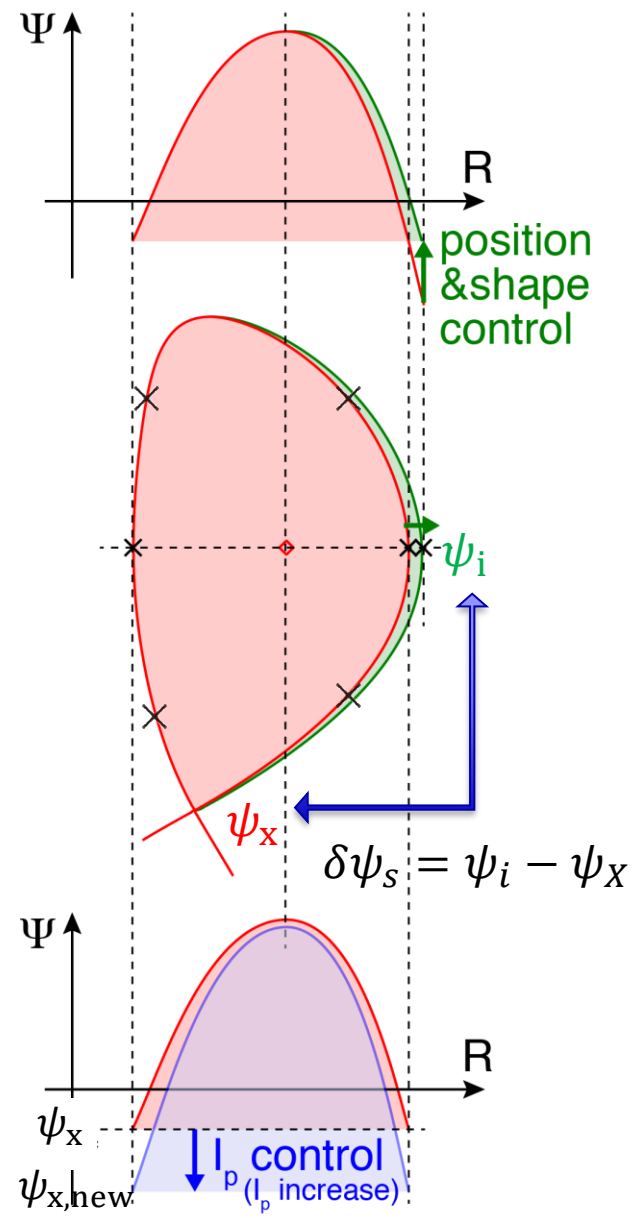
(Ip)  $\delta \psi_{\rm X}$ : Offset of all control points

$$\delta \boldsymbol{\psi} = \delta \boldsymbol{\psi}_{S} + \delta \boldsymbol{\psi}_{X}$$



Control eq.  $f_1(\delta \psi) = \delta I_c$  required change of coil current





#### **ISO-FLUX control**

(**Shape**)  $\delta \psi_{\rm S}$ : X-point and prescribed control points

(Ip)  $\delta \psi_{\rm X}$ : Offset of all control points

$$\delta \boldsymbol{\psi} = \delta \boldsymbol{\psi}_{S} + \delta \boldsymbol{\psi}_{X}$$

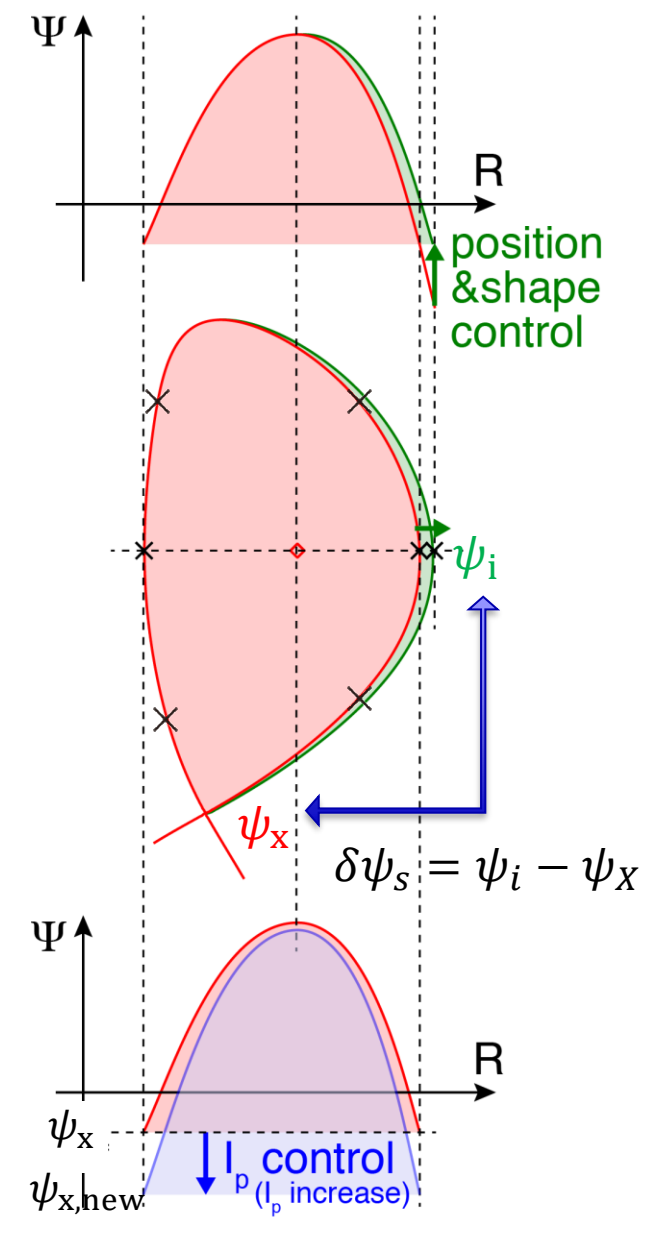


Control eq.  $f_1(\delta \psi) = \delta I_c$  required change of coil current



Circuit eq.  $f_2(\delta I_c) = V_c$  voltage command





#### **ISO-FLUX control**

(**Shape**)  $\delta \psi_{\rm S}$ : X-point and prescribed control points

(Ip)  $\delta \psi_{X}$ : Offset of all control points

$$\delta \psi = \delta \psi_{\rm S} + \delta \psi_{\rm X}$$



Control eq.  $f_1(\delta \psi) = \delta I_c$  required change of coil current



Circuit eq.  $f_2(\delta I_c) = V_c \leftarrow \text{voltage command}$ 

#### Adaptive voltage allocation scheme

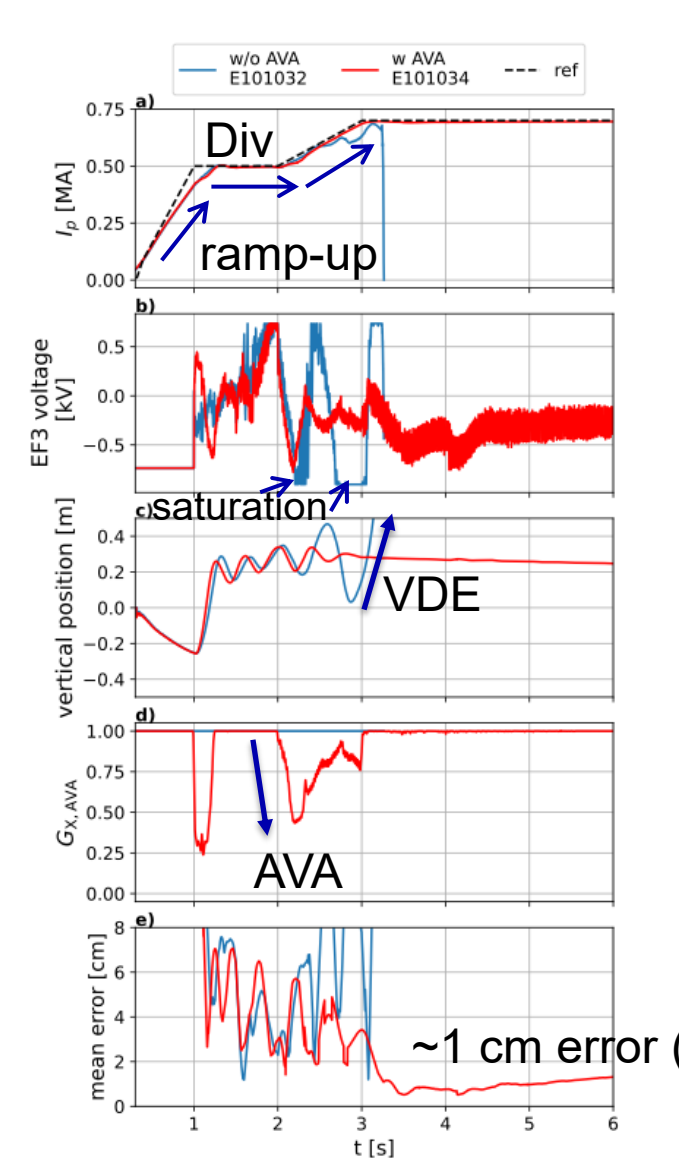
Inoue+, NF21, 23

$$G_{\rm X,AVA} \equiv \frac{|(f_1f_2)^{-1}(V_{\rm c,lim})|}{|\delta\psi_{\rm X}|} \Leftrightarrow {\rm Magnetic\ flux\ controllable\ under\ rated\ voltage\ limits}$$

$$\delta \psi_{\text{for control}} = \delta \psi_{\text{S}} + G_{\text{X,AVA}} \delta \psi_{\text{X}}$$

### **AVA** scheme resolved Ip/PS interference in IC



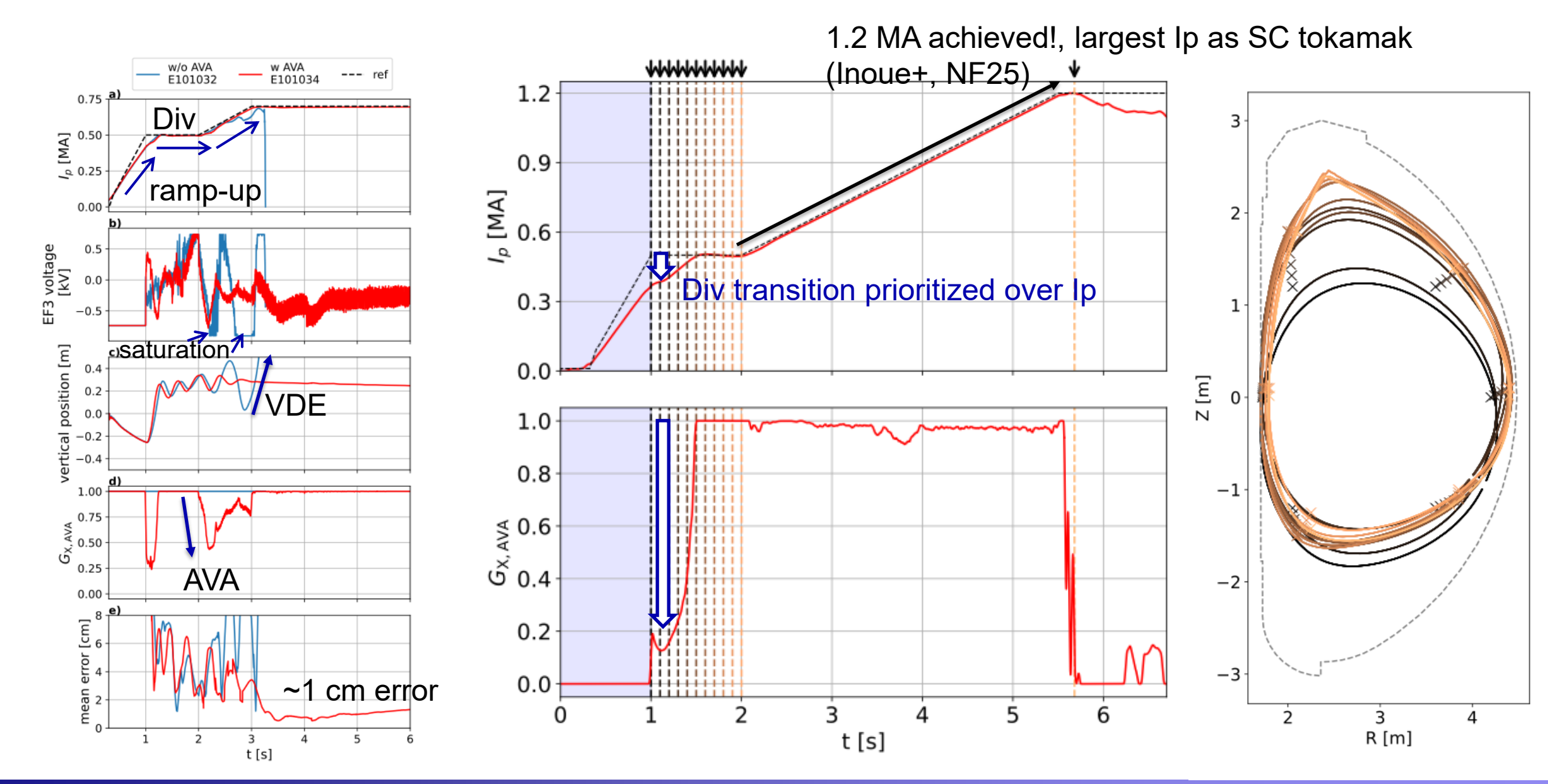


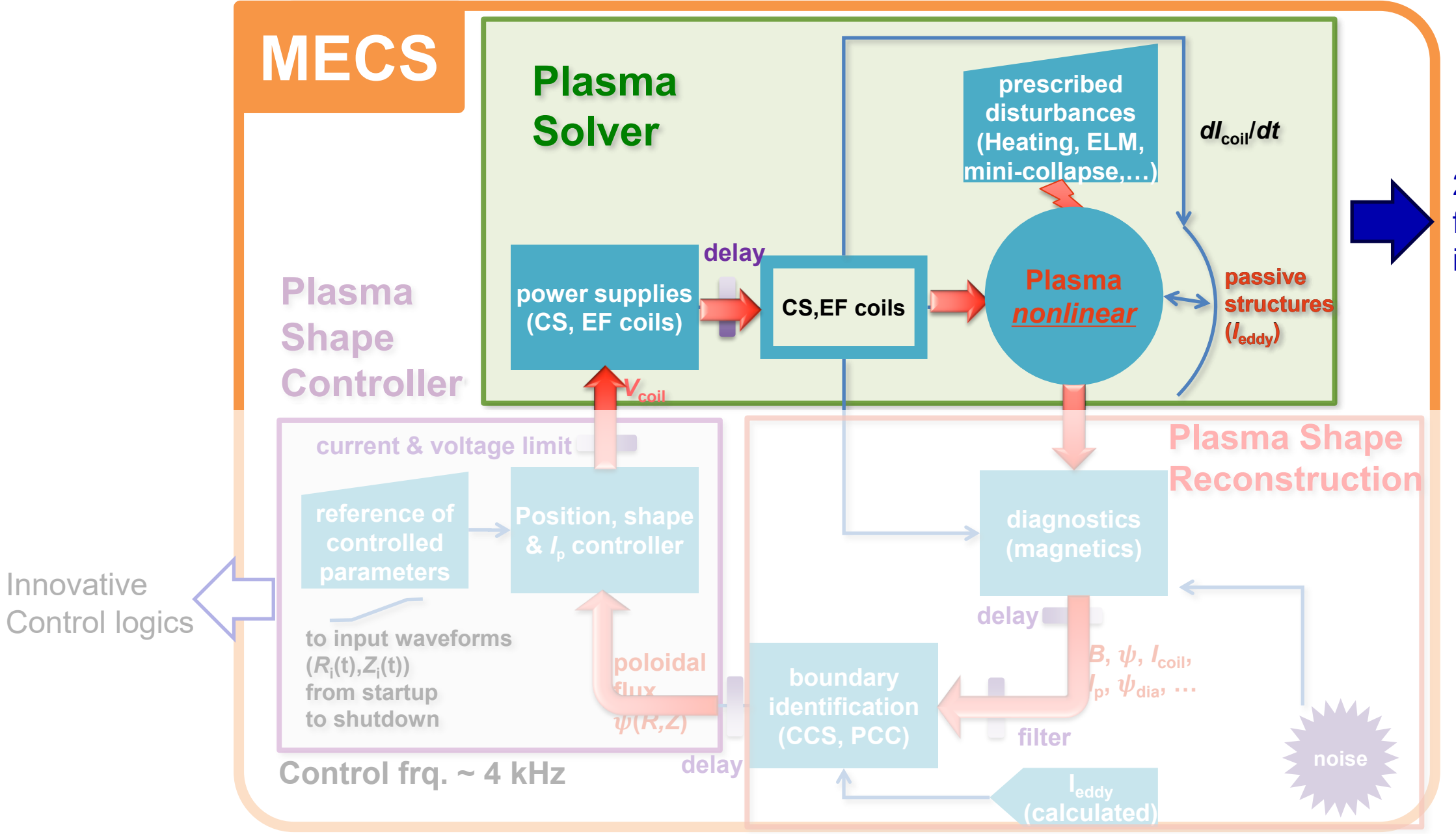
- Discharge: ramp-up to 500 kA → transition to divertor configuration → ramp-up to 750 kA
- Without AVA: oscillations during ramp-up and transition, leading to VDE
- With AVA:  $G_{X,AVA}$  resolved the voltage saturation and oscillations were suppressed, leading successful operation
  - Mean error < 2 cm</li>

~1 cm error (LCFS ⇔ Reference points)





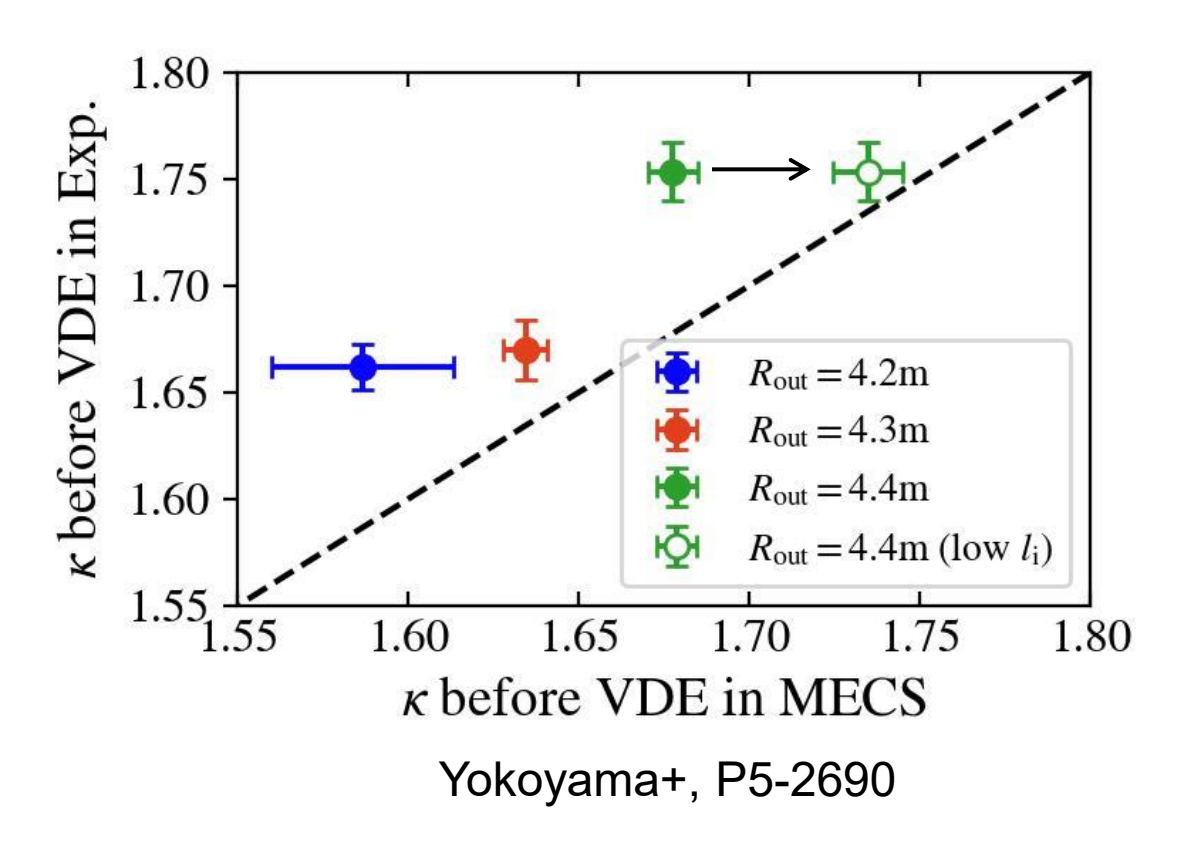




2.Key physics for vertical instability



### **Physics background of MECS**



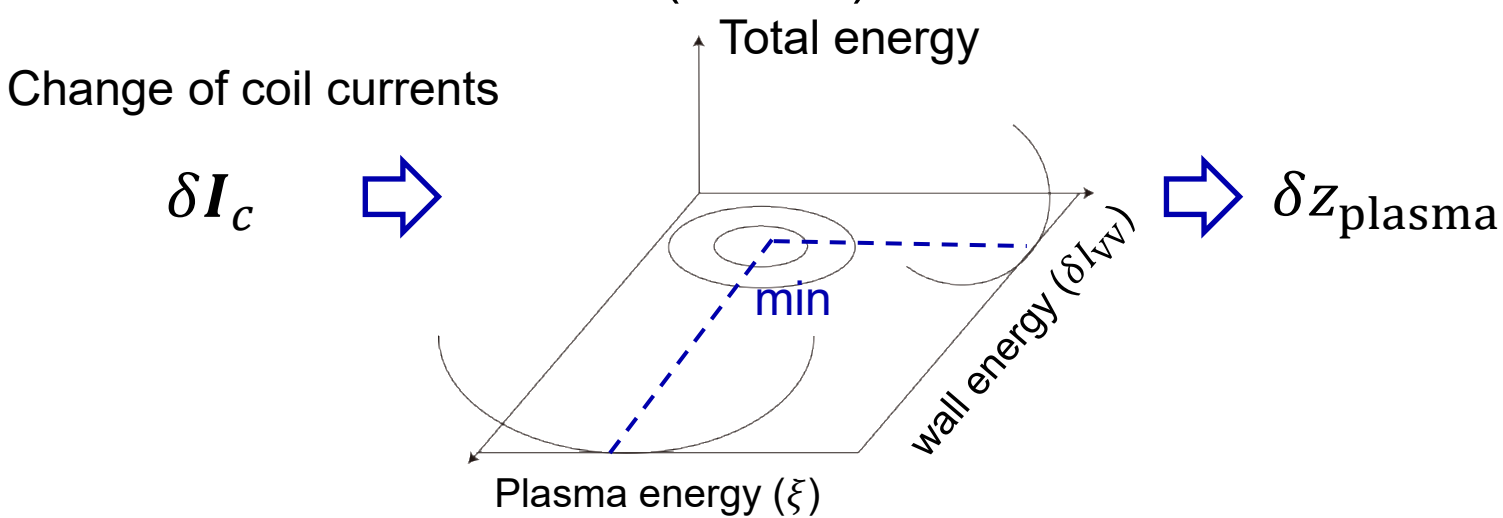
- From the energy principle, vertical instability (VI) appears as a minimum of plasma energy and wall/coil magnetic energy
  - Energy of plasma is proven to be perturbed
     Grad-Shafranov eq.<sup>1</sup>
- MECS, CREATE-NL, or DINA code can self-consistently simulate VI by coupling circuits equations with free-boundary Grad– Shafranov eq.
- MECS simulation captures the lower limit of accessible  $\kappa$  JT-60SA experiments went beyond it

Is self-consistent (but time-consuming) VI calculation indispensable for simulator?

<sup>&</sup>lt;sup>1</sup> J.P. Freidberg, A. Cerfon, and J.P. Lee, "Tokamak elongation – how much is too much? Part 1. Theory," J Plasma Phys **81**(6), 515810607 (2015).

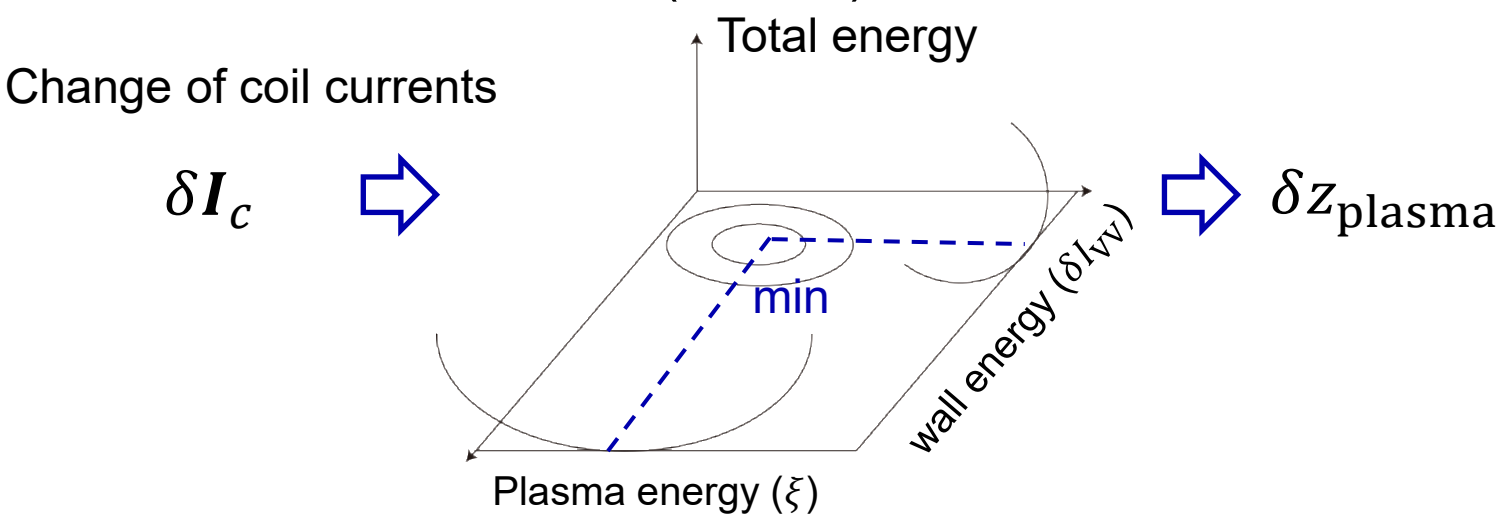
# Open loop response experiments for comparison between Linear and Nonlinear model

Nonlinear Model (MECS)



# Open loop response experiments for comparison between Linear and Nonlinear model

Nonlinear Model (MECS)



Linear Model

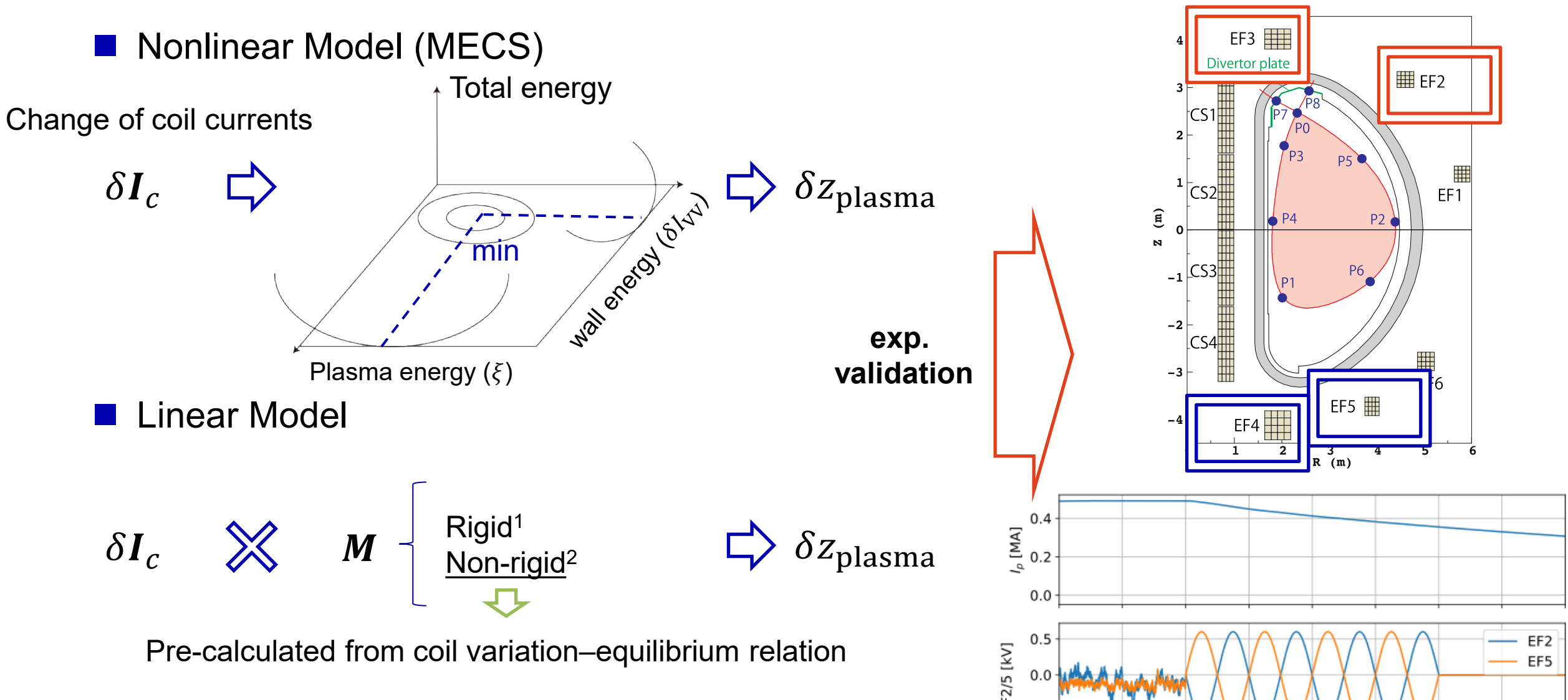
$$\delta I_c$$
  $\gtrsim$   $M$  Rigid<sup>1</sup>  $\delta z_{
m plasma}$ 

Pre-calculated from coil variation—equilibrium relation

<sup>&</sup>lt;sup>1</sup> A. Coutlis, *et al.*, Nucl Fusion **39**(5), 663–683 (1999).

<sup>&</sup>lt;sup>2</sup> A. Portone, Nucl. Fusion **45**(8), 926–932 (2005).

Open loop response experiments for comparison between Linear and Nonlinear model



2.00

2.25

2.75

t [s]

2.50

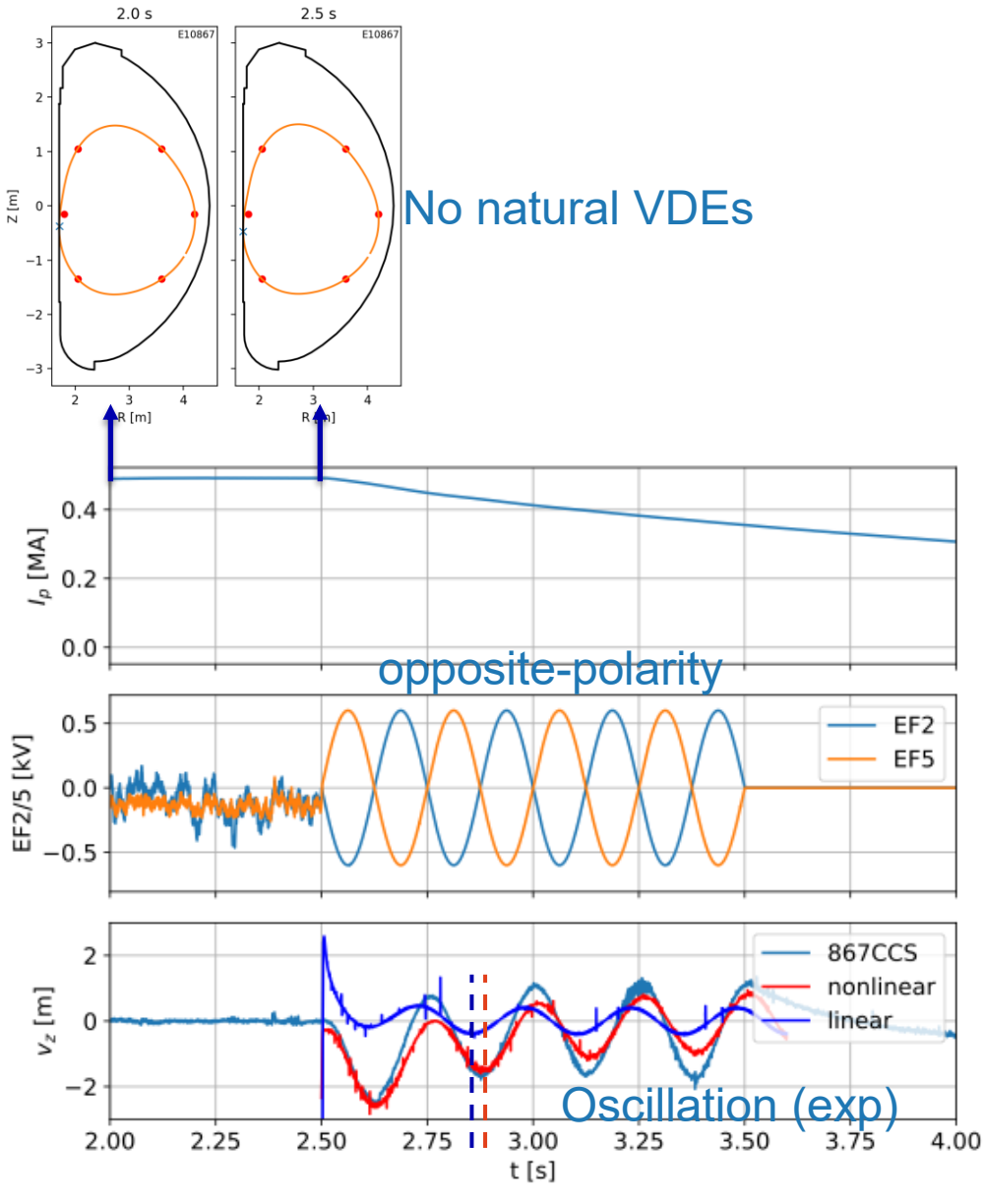
3.75

3.50

<sup>&</sup>lt;sup>1</sup> A. Coutlis, *et al.*, Nucl Fusion **39**(5), 663–683 (1999).

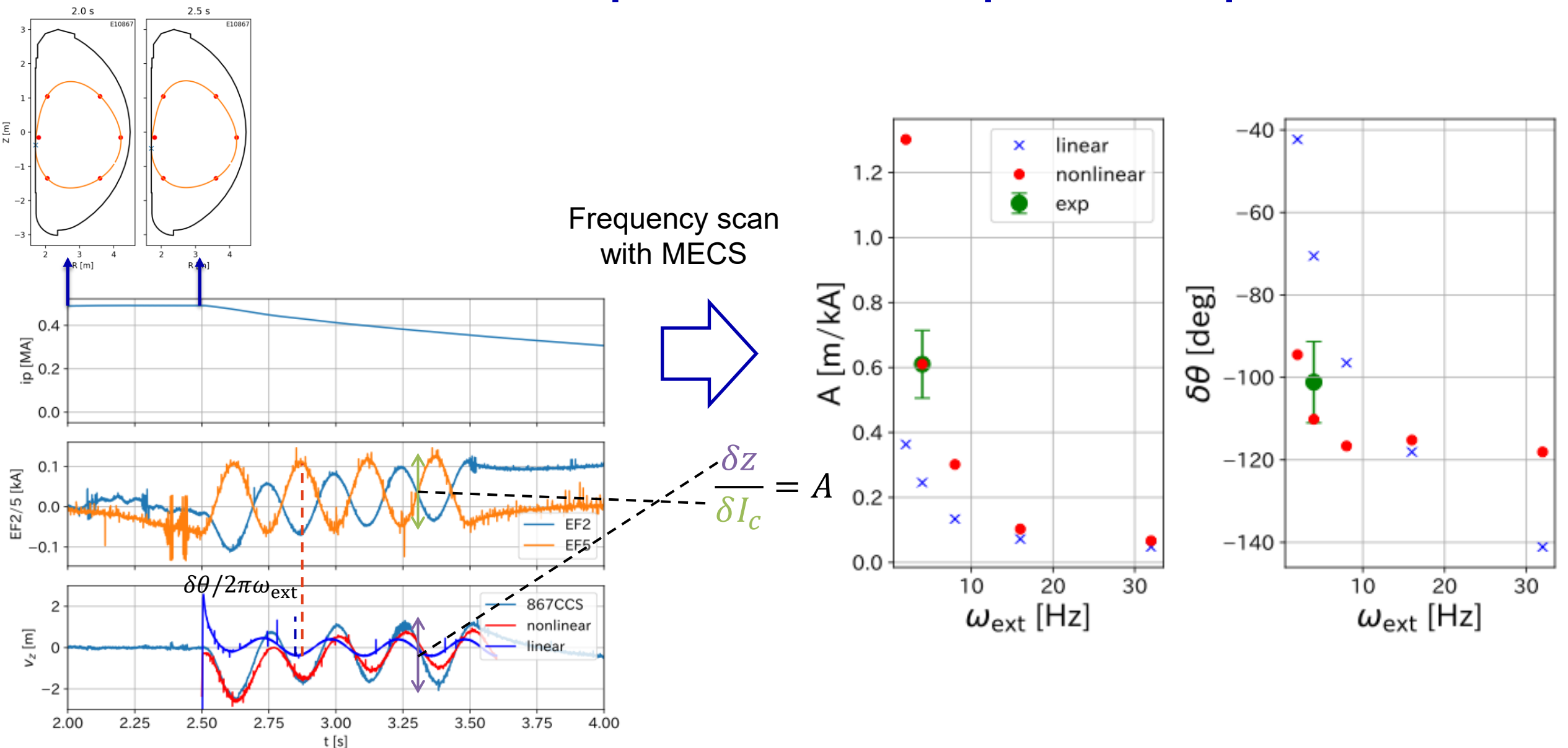
<sup>&</sup>lt;sup>2</sup> A. Portone, Nucl. Fusion **45**(8), 926–932 (2005).

### Nonlinear model reproduces both amplitude and phase



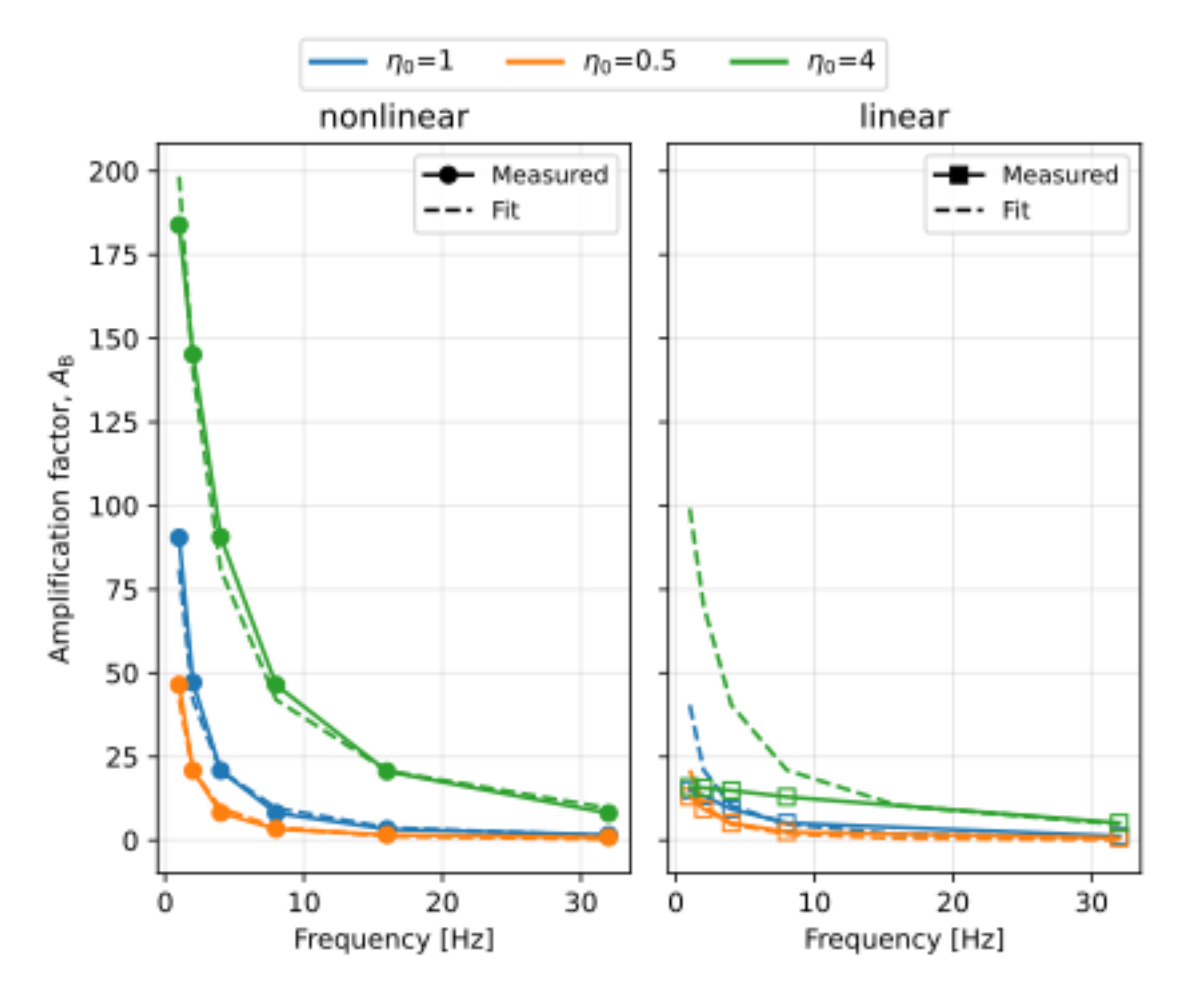
- Vertical oscillations were excited in response to change of EF coil current
- Simulations mimicking the experiment compared linear and nonlinear models
- Nonlinear model reproduced both amplitude and phase of the experiment well

### Nonlinear model reproduces both amplitude and phase





### Proposed RFA model qualitatively reproduces the nonlinear response



- Strong amplification at low frequency range is consistent with Resonant Field Amplification (RFA) of the stable n=0 resistive wall mode
- In simulations, wall resistivity was scanned from x1/2 to x4 to examine the response
- Following the RFA formulation¹:

$$\tau_W \frac{dB_S}{dt} = \gamma_0 \tau_W B_S + M^* B_{\text{ext}}$$

Including eddy-current shielding in  $B_{\rm ext}$  and assuming  $\delta z_{\rm s} \sim B_{\rm s}$ , the transfer gives:

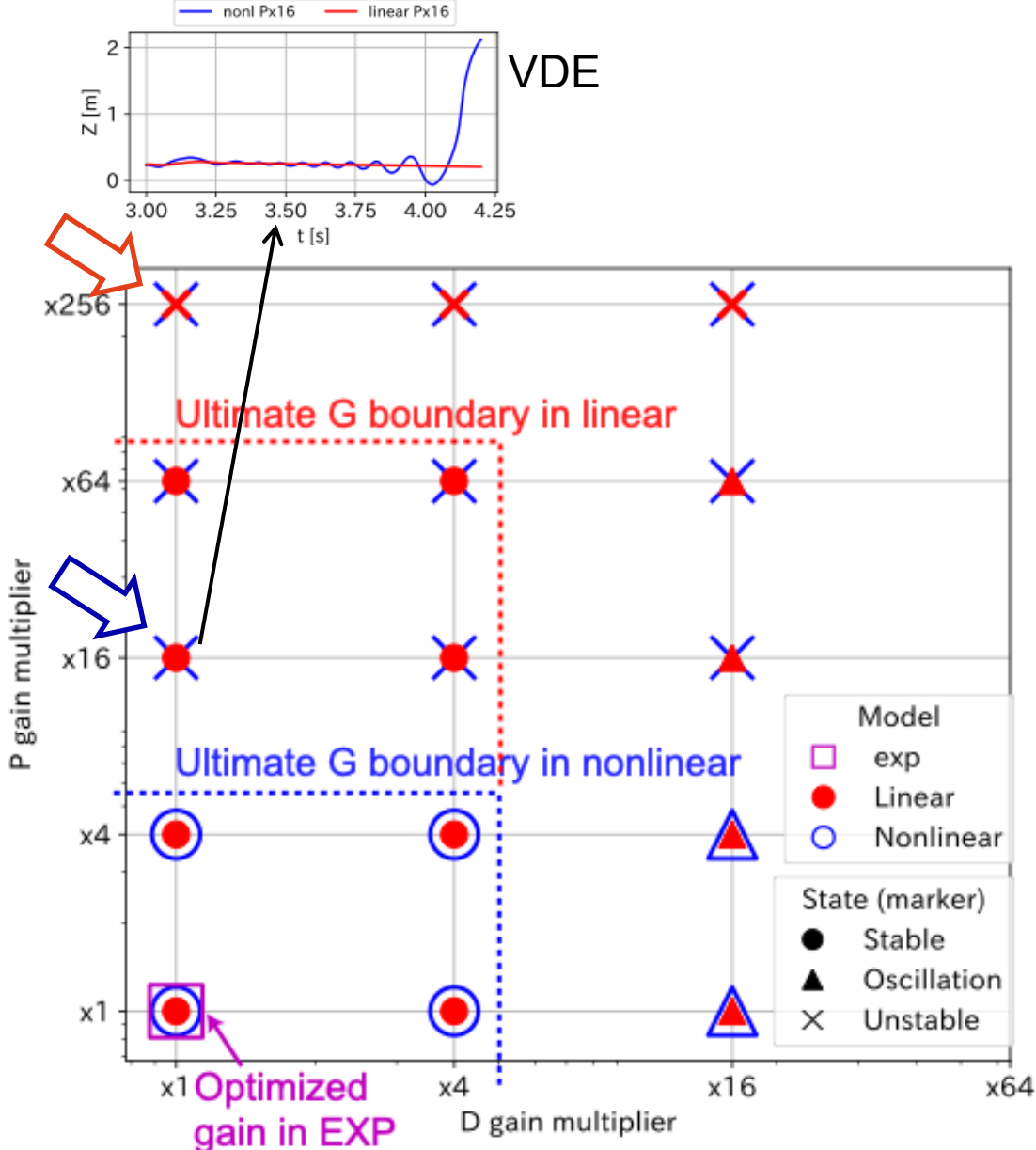
$$\frac{\delta z_{s}}{B_{\text{ext}}} \exp \delta \theta = \frac{A_{0}}{(1 + i\omega \tau_{W})(i\omega \tau_{W} - \gamma_{0})}$$

This model qualitatively **reproduces the** response with  $\tau_W = 450$  ms, and  $\gamma_0 = -20.7$  s<sup>-1</sup>

<sup>&</sup>lt;sup>1</sup> A.M. Garofalo, et al., "Sustained Stabilization of the Resistive-Wall Mode by Plasma Rotation in the DIII-D Tokamak," Phys Rev Lett 89(23), 235001 (2002).



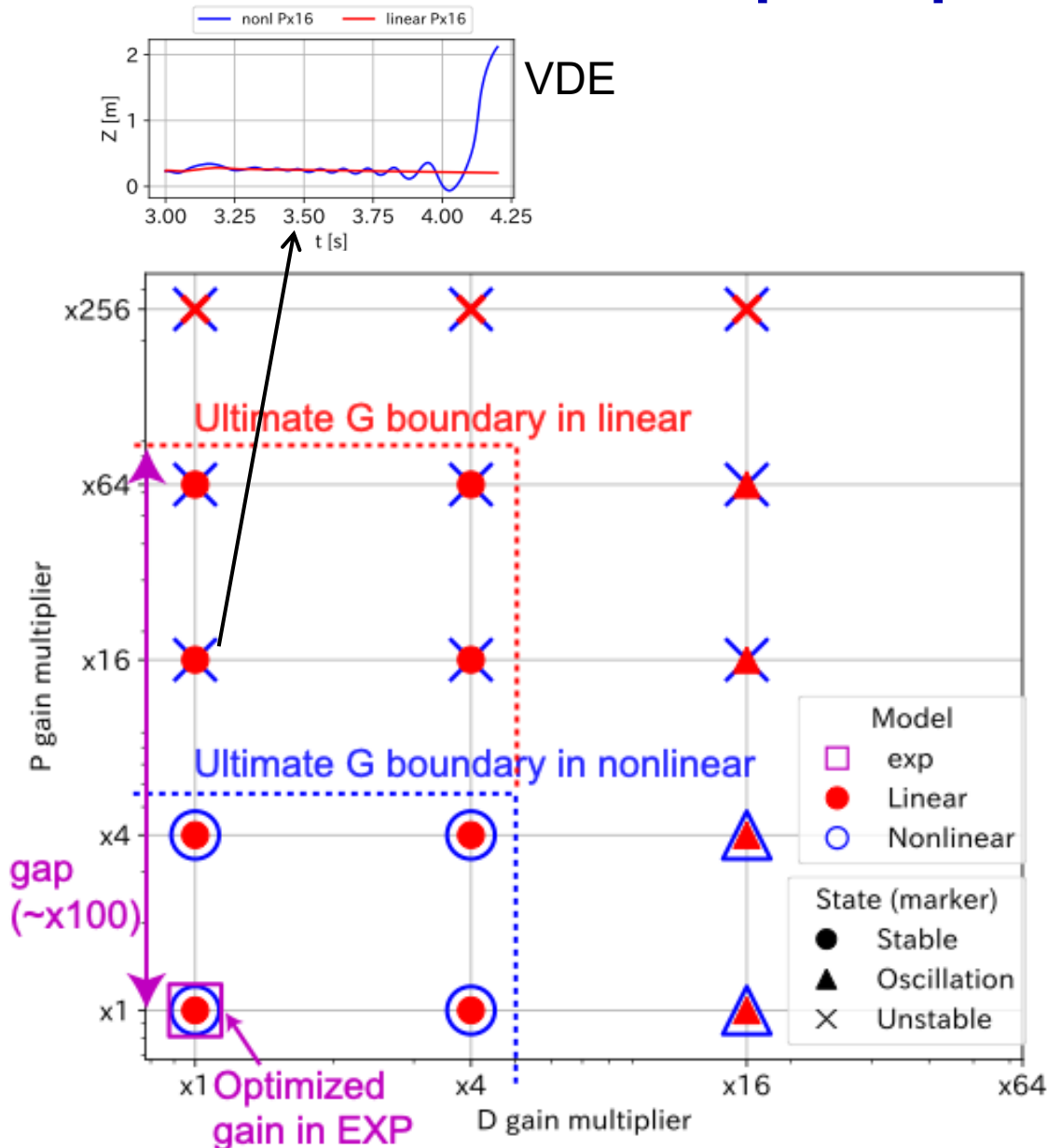




- Feedback control is applied in both models
- Optimized gain in exp. is unity
- Ultimate sensitivity gains are calculated by changing the PD gain
- Linear (red): unstable at ×256; Nonlinear (blue): unstable already at ×16



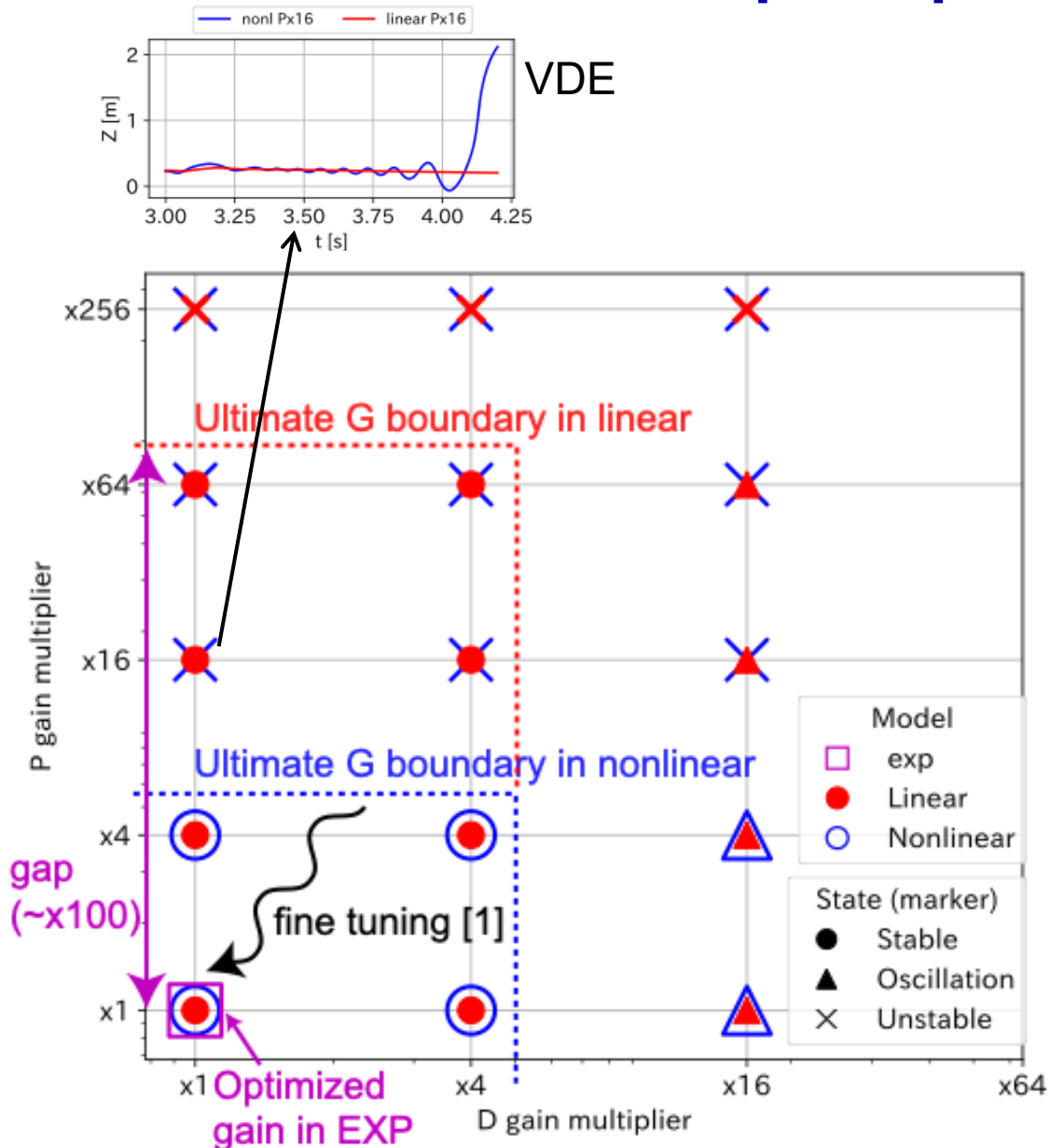




- Feedback control is applied in both models
- Optimized gain in exp. is unity
- Ultimate sensitivity gains are calculated by changing the PD gain
- Linear (red): unstable at ×256; Nonlinear (blue): unstable already at ×16
- Linear model: Ultimate sensitivity gains ≈ x100 higher → significant gap from the experiment

### **Closed-Loop Response: Importance of Nonlinearity**



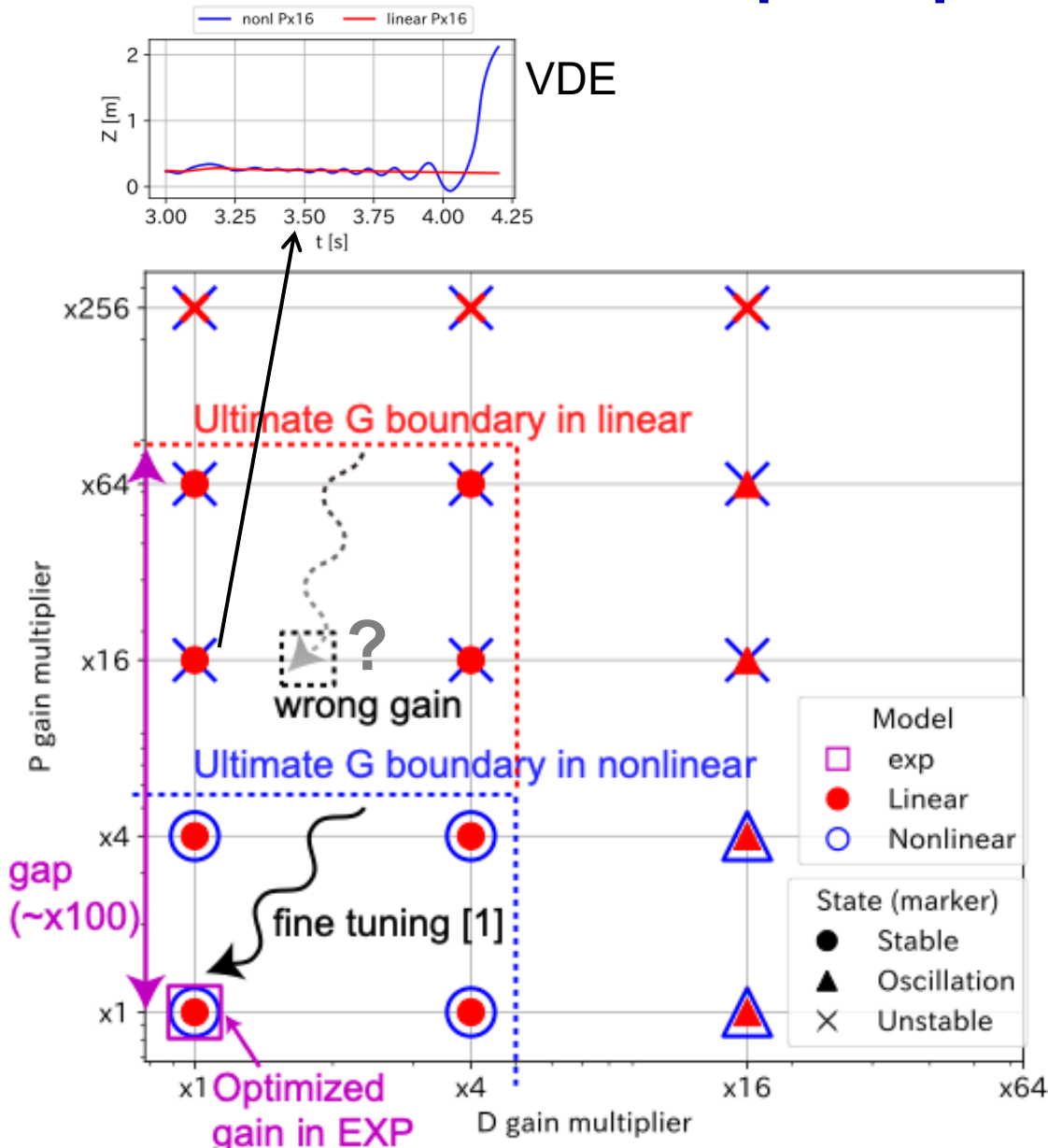


- Feedback control is applied in both models
- Optimized gain in exp. is unity
- Ultimate sensitivity gains are calculated by changing the PD gain
- Linear (red): unstable at ×256; Nonlinear (blue): unstable already at ×16
- Linear model: Ultimate sensitivity gains ≈ x100 higher → significant gap from the experiment
- Nonlinear model: Optimized ultimate sensitivity gains ≈ x4 experimental P, D gains
  - Optimal gain is the same order of the ultimate sensitivity gain → obtained by fine-tuning via frequency response with MECS [1]

[1] Kojima+, Nuclear Fusion 2025

### **Closed-Loop Response: Importance of Nonlinearity**



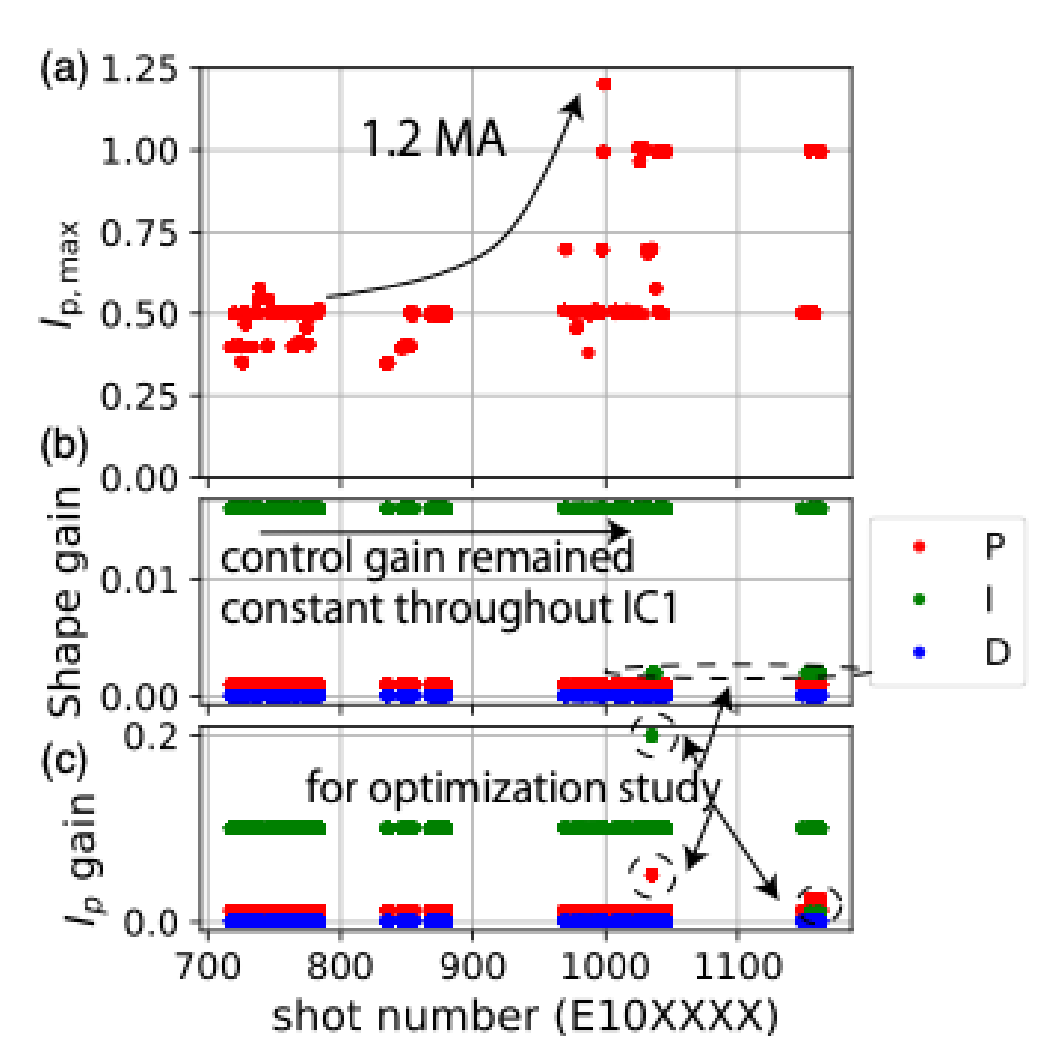


- Feedback control is applied in both models
- Optimized gain in exp. is unity
- Ultimate sensitivity gains are calculated by changing the PD gain
- Linear (red): unstable at ×256; Nonlinear (blue): unstable already at ×16
- Linear model: Ultimate sensitivity gains ≈ x100 higher → significant gap from the experiment
- Nonlinear model: Optimized ultimate sensitivity gains ≈ x4 experimental P, D gains
  - Optimal gain is the same order of the ultimate sensitivity gain → obtained by fine-tuning via frequency response with MECS [1]
- Under RFA, nonlinear model is essential

[1] Kojima+, Nuclear Fusion 2025



### **Summary and Future plan**



- JT-60SA's first operation achieved a smooth divertor transition, 1.2 MA plasma current, and a Guinnesscertified 160 m³ plasma volume, all using <u>pre-</u> <u>studied gains by MECS without modification</u>
  - MECS simulation captures the lower limit of accessible  $\kappa$  (Yokoyama+, P5-2690)

Key question: Why did the predictions work so well?

- Axisymmetric resonant field amplification a key physical process governing vertical instability was self-consistently solved in MECS, enabling preoptimization of control gains
- Toward OP2, direct control logic for  $\kappa \& \delta$ , together with the use of in-vessel coils & stabilization plates, will enable operation with  $\kappa > 2$  (Kojima+, P6-2716)







### **Nonlinear model**

#### **Loop 1** Plasma current update:

 $I_p^n \rightarrow I_p^{n+1}$  by Poynting's theorem and using external inductance as

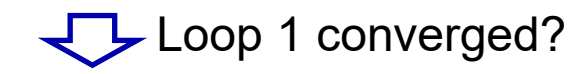
$$\frac{\partial}{\partial t} (\underline{L_p I_p} + \underline{\alpha C_E \mu_0 R_0 I_p}) + \dot{\psi}_{res} + \frac{\partial}{\partial t} (\sum_{coil} M_{cp} I_c + \sum_{vv} M_{vp} I_v) = 0$$

Plasma inductance Resistive flux consumption coil&vv mutual inductance

### Loop 2



- Magnetic axis update:  $x_{ax}^n \rightarrow x_{ax}^{n+1}$
- Imaginary quadrupole field update:  $\mathbf{B}_i^n \to \mathbf{B}_i^{n+1}$  with  $B_r(\mathbf{x}_{\mathrm{ax}}^{n+1}) = B_z(\mathbf{x}_{\mathrm{ax}}^{n+1}) = 0$
- Poloidal flux convergence:  $\psi_p^n \to \psi_p^{n+1}$  by  $-\Delta \psi = FF' + p'$
- Eddy currents update:  $I_v^n \to I_v^{n+1}$  by  $M_{vv} = \frac{\partial I_v}{\partial t} + M_{cv} = \frac{\partial I_c}{\partial t} + \frac{\partial (M_{pv}I_p)}{\partial t} + RI_v = 0$  vv, coil, and plasma multial inductances VV resistance
- Plasma current profile update:  $j_p^n(\psi) \to j_p^{n+1}(\psi)$  for  $\beta_p \& l_i$  convergence to prescribed values Loop 2 converged?





### **Linear Model**

Implemented following the non-rigid model [1]

$$L^*\dot{x} + Rx = V,$$
 Current center vertical displacement  $\longrightarrow z_P = Cx$ . (1)

where x is the vector of length  $N_c$  of mesh currents [8] and Vthe vector of voltages applied to the active coils. The elements of the  $N_c \times N_c$  modified inductance matrix  $L^*$  [2] and  $1 \times N_c$ output matrix C are:

$$L_{ij}^{*} \equiv L_{ij} - S_{ij} = \frac{\partial \psi_{i}^{(c)}}{\partial x_{j}} + \frac{\partial \psi_{i}^{(p)}}{\partial x_{j}},$$

$$C_{j} = \frac{\partial z_{p}}{\partial x_{j}},$$

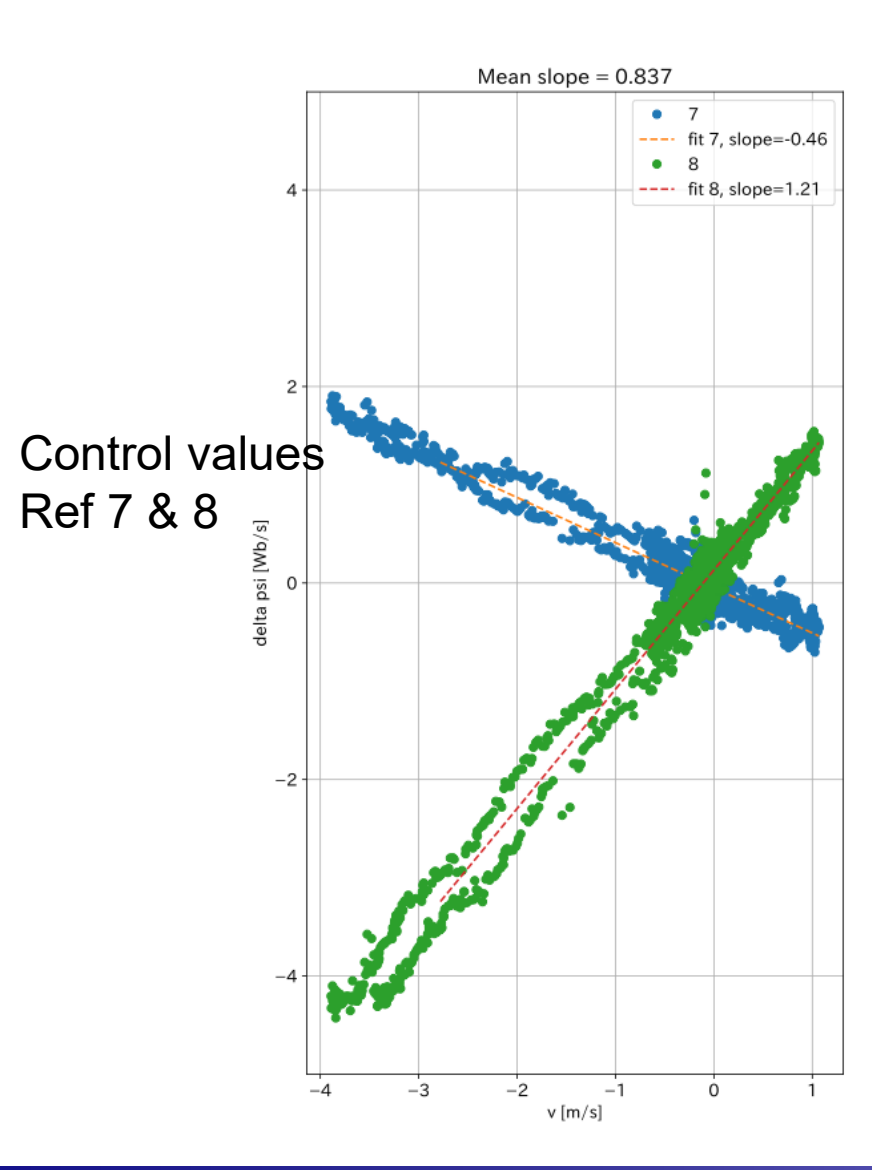
$$\uparrow$$
(2)

Computed from equilibrium changes due to coil variations

<sup>&</sup>lt;sup>1</sup> A. Portone, "The stability margin of elongated plasmas," Nucl. Fusion **45**(8), 926–932 (2005).



### Stabilization effect of controller (preliminary)



- $\Delta \Psi = \Psi_X \Psi_i$  (magnetic flux for control)
- Derivative control value:  $\frac{d}{dt}\Delta\Psi = \frac{\delta(\Psi_X \Psi_i)}{\delta t} \simeq \frac{d\psi}{dt} \equiv X$ , where  $\psi$  is a perturbed magnetic flux
- $T_W \dot{\psi} \gamma_0 \tau_W \psi = G \psi \to \tau_W \dot{X} \gamma_0 \tau_W X = G X$
- Controller compensate  $G_{\rm d} \frac{\delta(\Psi_X \Psi_i)}{\delta t}$  for 250 us
- If GX is constant during  $\delta t = 250$  us, from  $\int_0^{\delta t} GX dt = G_{\rm d} \frac{\delta(\Psi_X \Psi_i)}{\delta t}$

$$G = G_d/\delta t = 10^{-4} \times 4000 = 0.4$$

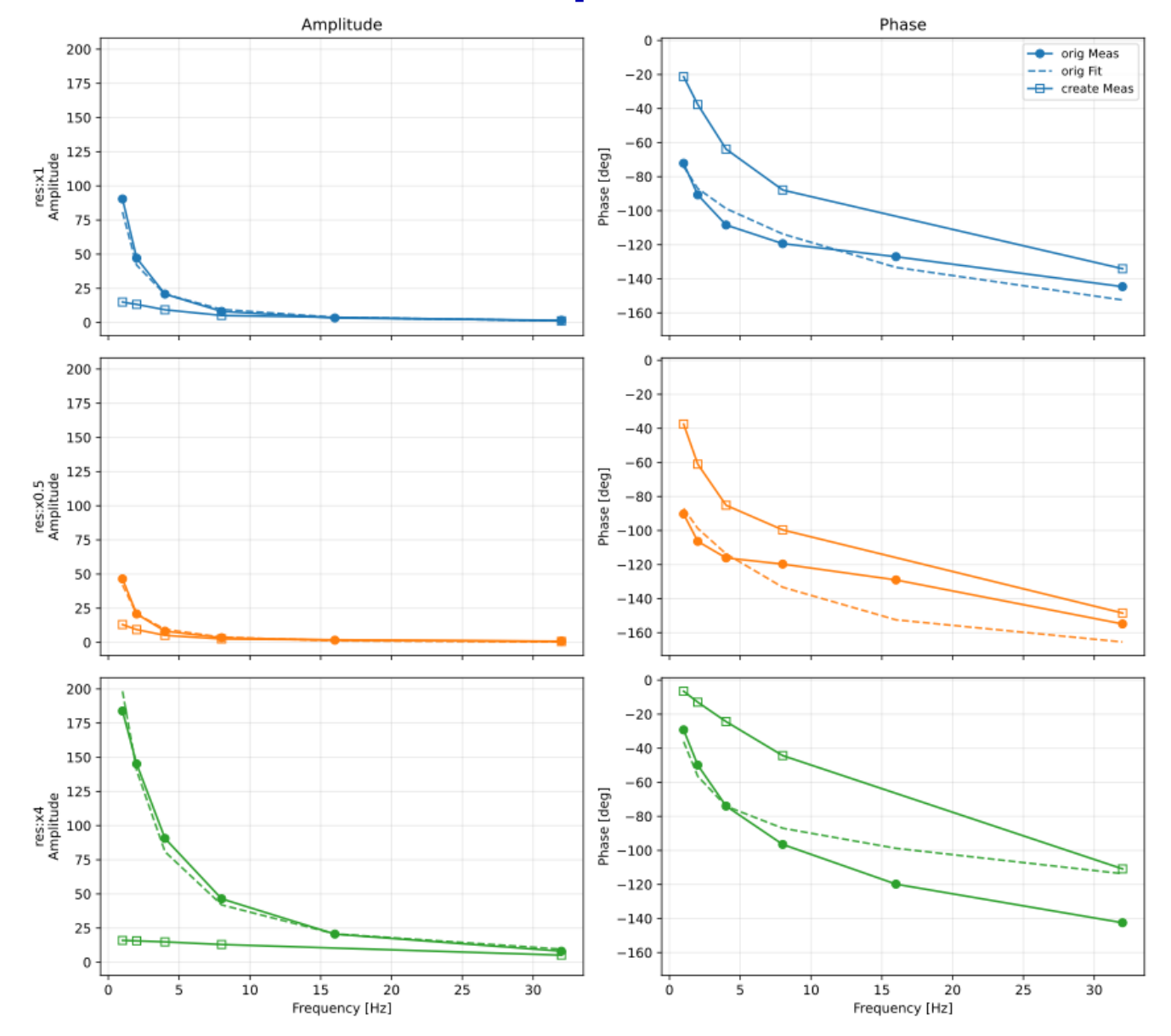
From the figure X corresponds to the vertical velocity, thus G can be compared to  $\gamma$  of vertical instability,

$$G = 0.4 \ll \gamma_0 \sim 50$$

- $\dot{X} \sim v$
- Experimentally applied gains and observed growth rate strongly indicates that the controller has the stabilization effect against vertical instability



### with phase



# Largest Plasma Volume 160 m<sup>3</sup> was achieved by increasing elongation



Errors are quite small < 1% => small drifts & noises

